

Attenuating non-compressional energy on vertical motion sensors using rotational data

Hassan Masoomzadeh*, Fons ten Kroode, Tim Seher, Mohammad Akbar Hosain Zuberi (TGS), Alexander Kritski, Harald Westerdahl, Åsmund Sjøen Pedersen, Mark Thompson (Equinor), Nick Bernitsas, Phil Behn, Philip Baltz (Exion Technologies)

Summary

In this paper we investigate the use of rotational acceleration measurements for attenuating non-compressional, or “non-P” energy on vertical particle motion records from Ocean Bottom Node (OBN) data. This energy consists of mode converted shear reflections and interface waves traveling over the ocean bottom. We deployed three OBNs equipped with a new 6C sensor, capable of measuring translational and rotational acceleration, and a hydrophone, during a multi-client OBN survey in the Gulf of Mexico. The survey was shot with two source vessels, each towing three airgun arrays, which were firing in a dithered manner. The first processing step was therefore to deblend all six components of the data. Subsequently, we compared a model for the non-compressional energy on the vertical particle acceleration data estimated from the rotational components against a model obtained from pressure and vertical particle acceleration data by thresholding in the curvelet domain. The results show that the attenuation of non-compressional energy based on rotational data has the potential to outperform the traditional curvelet domain approach.

Introduction

The new ‘Ksphere’ six component (6C) sensor (Pedersen et al., 2023) measures both translational and rotational particle acceleration. The sensor consists of an inertial spherical mass suspended inside a rigid cubic frame. It has six piezoelectric crystals, mounted on sensor blades between frame and sphere, one on each face of the cube. The blades and crystals are only sensitive to motion of the frame in the direction of the arrows in Figure 1. Since the frame is rigid, translational motion can be obtained by summing signals from sensors on opposing faces, rotational motion by subtracting these signals.

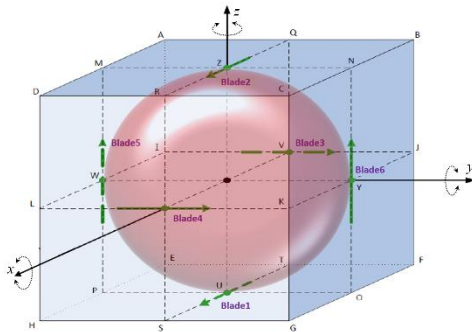


Figure 1: A schematic drawing of the ‘Ksphere’ 6C sensor.

A significant advantage of OBN data is the facilitation of up-and downgoing wavefield separation. This is based on the fact that a hydrophone is an omnidirectional receiver, which is insensitive to the direction which an incoming pressure pulse comes from, whereas geophones and accelerometers are unidirectional receivers. Hence, an upgoing pressure pulse is observed as a positive event in both hydrophone and vertical geophone or accelerometer, while a downgoing pressure pulse generates a positive signal in the hydrophone and a negative signal in a vertical sensor. Therefore, a summation of those signals will approximately annihilate the downgoing pulse, while a subtraction will approximately annihilate the upgoing pulse.

In practice, there are many details to be considered to achieve a successful up-down separation of the wavefield, for example obliquity correction and instrument calibration. More importantly, the presence of non-compressional events in the form of shear body waves and interface waves on vertical geophone records can pose significant challenges (Paffenholz et al., 2006a, 2006b). Over the years, a variety of processing techniques have been developed to attenuate non-compressional energy on vertical geophone records using thresholding in various transform domains, such as the tau-p domain (Craft & Paffenholz, 2007; Poole et al., 2012), the wavelet domain (Peng et al., 2013; Ren et al., 2020), and the curvelet domain (Yang et al., 2020; Kumar et al., 2021; Ren et al., 2022). These methods can fail, however, in case of insufficient discrimination between compressional and non-compressional events in this domain. This paper investigates the use of rotational acceleration data measured by the new 6C sensor to attenuate non-compressional energy on vertical accelerometers.

Theory

We start with the standard Helmholtz decomposition of the particle acceleration wavefield \vec{a} into scalar and vector potentials ϕ and \vec{A} ,

$$\vec{a} = \nabla \phi + \nabla \times \vec{A}. \quad (1)$$

Using the gauge condition $\nabla \cdot \vec{A} = 0$, and the fact that the curl of a gradient is zero, the angular acceleration vector takes the form

$$\vec{\alpha} := \frac{1}{2} \nabla \times \vec{a} = -\frac{1}{2} \Delta \vec{A}. \quad (2)$$

Attenuating non-compressional energy on vertical motion sensors using rotational data

Here Δ denotes the Laplacian. Assuming that the earth is homogeneous and isotropic in a layer below the water bottom, the vector potential \vec{A} in that layer satisfies the wave equation

$$\frac{1}{c_s^2} \partial_t^2 \vec{A} = \Delta \vec{A}, \quad (3)$$

with c_s representing the shear wave velocity. It follows that

$$\vec{A} = -2c_s^2 \partial_t^{-2} \vec{a}. \quad (4)$$

The symbol ∂_t^{-2} in this formula stands for double integration with respect to time. The non-compressional part of the acceleration wavefield can therefore be written as

$$\vec{a}^S := \nabla \times \vec{A} = -2c_s^2 \partial_t^{-2} \nabla \times \vec{a}. \quad (5)$$

Its vertical component reads

$$a_z^S = -2c_s^2 \partial_t^{-2} (\partial_x \alpha_y - \partial_y \alpha_x). \quad (6)$$

In the (k_x, k_y, ω) -domain, this can be written as

$$\hat{a}_z^S = \frac{2c_s^2}{\omega^2} (-ik_x \hat{\alpha}_y + ik_y \hat{\alpha}_x). \quad (7)$$

At the water bottom, the wavefield is the sum of up- and downgoing P and S body waves and interface waves. Non-compressional interface waves come in the form of Scholte and leaky Rayleigh waves on the one hand and Love waves on the other hand. The former consist of interfering P-SV waves, which decay exponentially in the water column and in the solid earth (Scholte, 1958). The latter consist of a system of horizontally propagating SH waves, and exhibits rotational movement around the vertical axis, but no translational movement in the vertical direction. They can therefore be ignored for the purpose of up-down separation. Reflection and transmission coefficients, and velocities of the interface waves can be determined by imposing standard interface conditions. The velocity of the non-compressional interface waves will become frequency dependent for a non-constant earth model. With that qualification, the non-compressional part of all these waves satisfies equation (7).

The formulas above show that, given the assumption of a homogeneous and isotropic shallow layer, it suffices to know the horizontal components of rotational acceleration (α_x and α_y) and their horizontal derivatives with respect to receiver coordinates to compute non-compressional energy on the vertical accelerometer a_z . The problem with this is that a typical OBN survey is sampled too sparsely in the receiver coordinates to compute these derivatives. In a

laterally homogeneous earth, we can replace them by derivatives with respect to the source coordinates, in which an OBN survey is typically well sampled. Replacing Fourier transforms with respect to receiver coordinates in the formulas above by their source domain counterparts, will therefore provide an approximation of the non-compressional energy on the vertical component, which is correct for the case of a laterally homogeneous earth. One can correct for errors related to this approximation by adaptive subtraction from the full acceleration wavefield.

Example

We tested three OBNs equipped with the new 6C sensor and a hydrophone during a multi-client sparse nodal survey in the Gulf of Mexico, which used normal 4C OBNs (3C geophone plus hydrophone) for production purposes. Our test data set therefore consists of three 7C nodes, which recorded all shots in the production survey. This survey was shot using two vessels firing triple airgun arrays in a dithered manner. We selected a subset of the sail lines, acquired when only one of the source vessels was operating. For these sail lines, only self-blending of the three airgun arrays plays a role. The results of deblending the six translational and rotational components of one of the test nodes are shown in Figure 2.

We subsequently tested adaptive subtraction of the horizontal rotational components in the (k_x, k_y, ω) -domain. As explained in the previous paragraph, this can only be done approximately, by interchanging Fourier transforms with respect to receiver and source coordinates, which is only correct for a laterally homogeneous subsurface. In order to do this, we had to first rotate all six components measured by the new sensor to inline, crossline and vertical directions. By doing so, the rotational components correspond to rotational acceleration around these directions. We have tested both adaptive subtraction of the right hand side of equation (7) and adaptive subtraction of the two horizontal rotation components $\hat{\alpha}_x$ and $\hat{\alpha}_y$. In the former case, only one filter is derived. In the latter case, two filters are derived to minimize the energy in the remainder, which provides the algorithm with more flexibility to mitigate errors induced by approximations in the algorithm. It was found that the latter approach led to the best results. In Figure 3, we show these results and compare them against a conventional curvelet domain scheme to separate compressional and non-compressional energy.

Figures 3a and 3b show the hydrophone and vertical acceleration records. The latter clearly contains energy, which is not present on the hydrophone. It is this energy that needs to be attenuated before up-down separation of the vertical wavefield.

Attenuating non-compressional energy on vertical motion sensors using rotational data

The conventional approach uses both vertical acceleration and hydrophone data and compares them in the 2D curvelet domain. Events that are present in the vertical component but absent in the hydrophone records are identified and are subsequently removed. The curvelet domain approach is quite effective and has been adopted by the industry, yet it may fall short near the apex where there is insufficient discrimination between P and non-P events in the curvelet domain. This effect is apparent when comparing the result after subtraction in Figure 3c with the hydrophone data in Figure 3a. The high amplitudes inside the black ellipse in Figure 3c are seen on the vertical record, and not on the hydrophone. We interpret these amplitudes as residual non-P energy. At the same time, the energy identified as non-P energy in the curvelet domain clearly has some P leakage, see Figure 3d.

Figures 3e and 3f show the results of adaptive subtraction of the horizontal rotational components and the model for the non-P wave energy as derived in this manner. While some

non-P energy residual can be seen on Figure 3e, the result at the apex is better than the curvelet domain one in Figure 3c.

Conclusions

We examined a new generation of ocean bottom seismic data acquired by nodes consisting of a conventional hydrophone and six component sensors measuring translational and rotational particle motion. We showed that all components can be successfully deblended, and that the horizontal rotational components can be used to estimate a model for the non-compressional energy on vertical accelerometers, which can be subtracted from the vertical component to facilitate separation of up- and downgoing wavefields. This leads to better results than a conventional curvelet domain method.

Acknowledgements

The authors would like to thank TGS for giving their permission to publish these results.

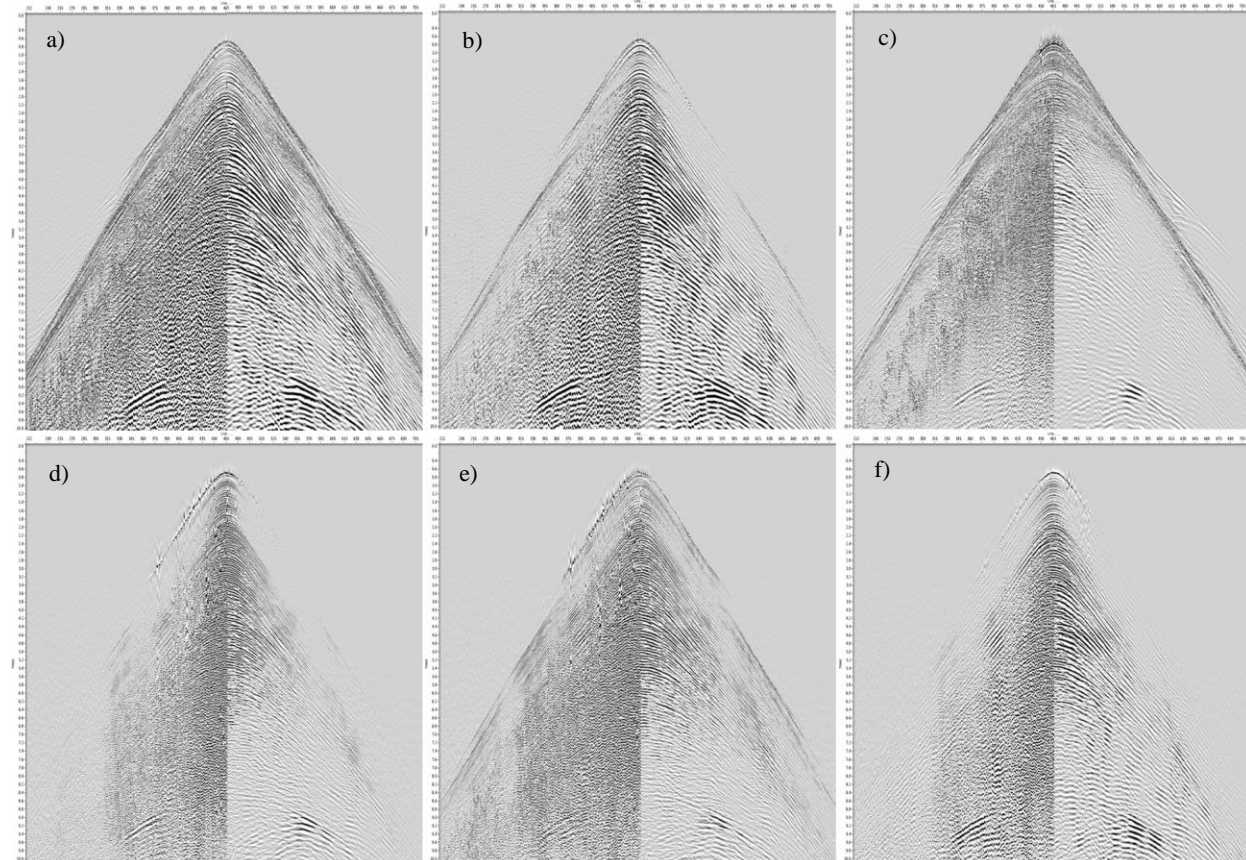


Figure 2: Six components recorded by a Ksphere sensor before deblending (left halves) and after deblending (right halves). a) to c) Inline, crossline and vertical components of translational acceleration. d) to f) Same components for rotational acceleration.

Attenuating non-compressional energy on vertical motion sensors using rotational data

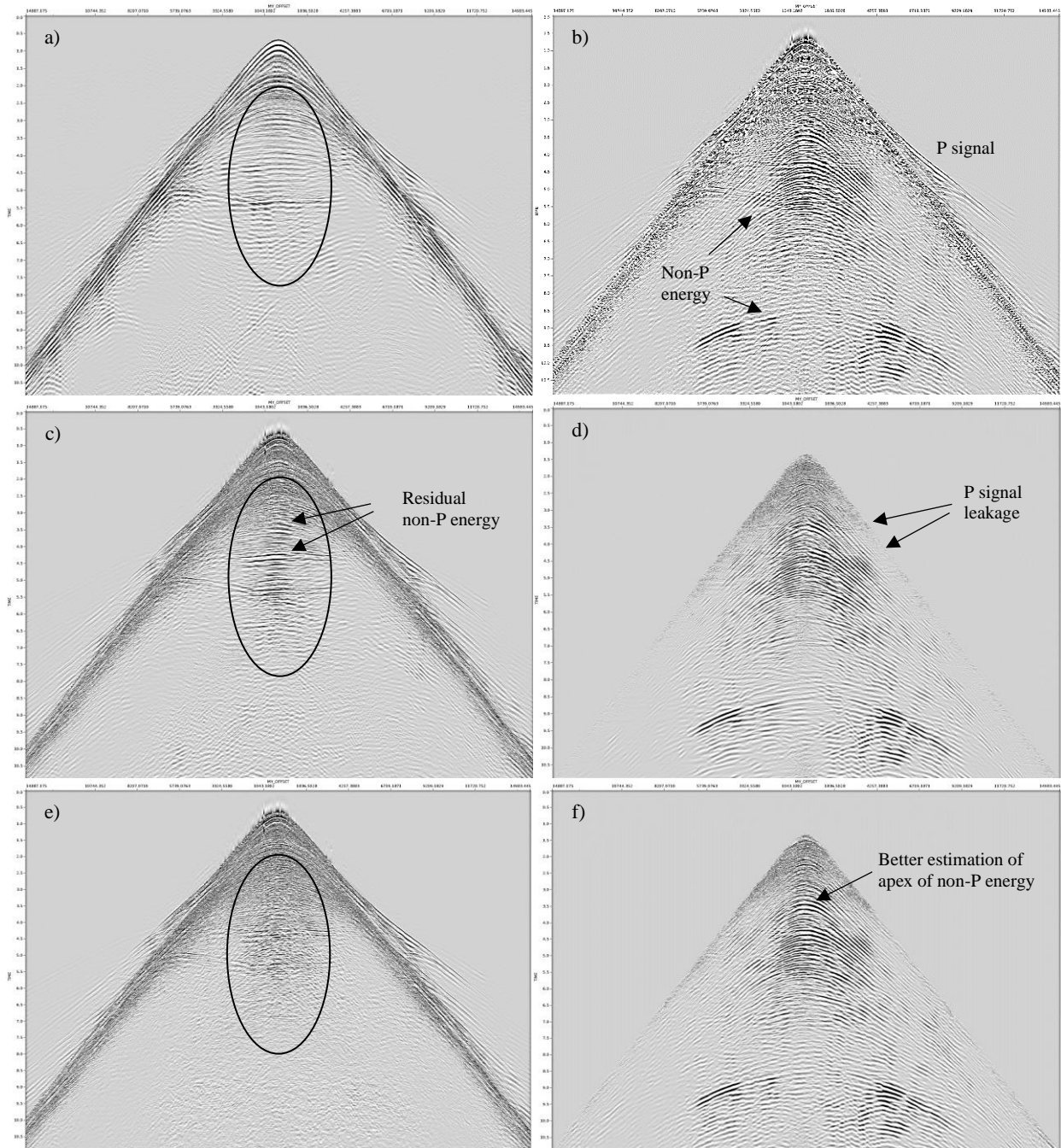


Figure 3: a) Hydrophone data. b) Vertical acceleration data containing both P and non-P events. c) Vertical component after curvelet domain subtraction of non-P energy, where based on comparison with (a) some non-P energy can be identified. d) non-P model estimated using the curvelet domain approach, where some P leakage and lack of non-P energy at the apex is observed. e) Vertical component after denoising based on horizontal rotational components, which looks more similar to the P data in (a). f) Non-P model from rotational data, where P leakage is absent and non-P events are more energetic than in (d).